Time-dependent photoluminescence of InP:Fe

P. B. Klein, J. E. Furneaux, and R. L. Henry
Naval Research Laboratory, Washington, D.C. 20375
(Received 12 September 1983)

The time dependence of the $^5T_2 \rightarrow {}^5E$ photoluminescence transition of Fe^{2+} in InP has been measured as a function of temperature for a well-characterized series of Fe-doped samples ranging from n type to semi-insulating. The observed time dependences can be fitted over a wide range of temperatures by a relatively simple model that accounts for the relaxation of the system back to the equilibrium (dark) condition. The magnitude of the low-temperature electron capture cross section by the neutral Fe^{3+} center ($\sigma_n > 5\times10^{-16}$ cm^2 at 5 K) was found to be much larger than expected and exhibited a marked decrease with increasing temperature up to 29 K. This has been interpreted in terms of a two-step capture process involving a shallow level. The low-temperature capture cross section for holes ($\sigma_p \approx 2\times10^{-17}$ cm^2) and the lifetime of the $^5T_2 \rightarrow {}^5E$ excited state ($\tau_0 \approx 11$ μsec) were also determined. The latter quantity decreases dramatically with temperature due to $^5T_2 \rightarrow {}^5E$ multiphonon relaxation. It was also determined that an Auger process recently discussed by Langer can be important during the exciting pulse in inducing $^5T_2 \rightarrow {}^5E$ nonradiative transitions.

I. INTRODUCTION

The Fe impurity in InP introduces a deep level which compensates residual donors, thus forming semi-insulating (SI) material.[1] The singly ionized acceptor state Fe^{2+} ($3d^6$) exhibits two crystal-field-split levels within the forbidden gap which are separated by 0.35 eV. Radiative transitions between the excited ($^5T_2$) and ground (^5E) states are often observed in photoluminescence (PL) measurements[2-7] as a characteristic set of four sharp, closely spaced ($\approx$14-cm^{-1}) emission lines, which result from higher-order spin-orbit splittings of the ground state. Recently,[8] we have reported the observation of laser oscillations near 3.5 μm due to the $^5T_2 \rightarrow {}^5E$ internal transitions of Fe^{2+} in n-InP:Fe. This represents the first observation of laser oscillations from the internal transitions of an impurity in a semiconductor, where excitation via electrical injection is a possibility. We also suggested a relatively simple mechanism for the observed laser oscillations involving electron capture by the neutral acceptor state Fe^{3+} ($3d^5$). A more detailed understanding of the processes dominating the kinetics of this system is of interest both from a fundamental point of view as well as for application to the problem of laser oscillations from deep impurities. Toward that end, we have studied the kinetics of the excitation and recombination processes associated with both charge states (Fe^{3+} and Fe^{2+}) of the Fe center by peforming time-dependent PL measurements on a carefully characterized set of InP:Fe samples. The results of these measurements suggest specific models that describe the system kinetics after the exciting pulse and also provide information about the magnitudes of the important system parameters and the dominant processes occurring during the exciting pulse.

The study of the Fe impurity in III-V compounds has been the subject of many investigations over the past several years. Much of this literature has been reviewed in a recent article by Bishop.[9] Excitation of the 0.35-eV PL transition requires that some of the Fe centers must be populated in the excited $^5T_2$ level of the Fe^{2+} charge state, $(Fe^{2+})^*$. Since the energy for the direct internal excitation of the Fe^{2+} ground state to higher-lying internal levels is expected to be considerably larger than the Fe^{2+} photoionization energy, this process is not considered to be important in exciting the 0.35-eV PL. Therefore the Fe^{2+} excited state must be created from the equilibrium charge states Fe^{3+} and Fe^{2+} (^5E) by processes that change the charge state of the center. Several previous studies have dealt with specific excitation mechanisms associated with the Fe center in various III-V semiconductors. Bishop *et al.*[4] suggested on the basis of the weak cw PL intensity observed in n-type material compared to that in SI samples that the Fe^{2+} is excited via electron capture by Fe^{3+}. This was corroborated by Tapster *et al.*[6] and by Leyral *et al.*,[7] where it was suggested[6,7] that the weakness of the PL intensity in n-type material might also be explained by a competing, unspecified Auger process. Leyral *et al.* compared the PL excitation (PLE) spectra for n-type and SI samples with the spectral dependence of the photoionization cross sections[10] for electrons and holes at the Fe center. They determined that the excitation of PL *with below-gap light* proceeded predominantly via the photoionization processes $Fe^{2+} \rightarrow Fe^{3+} + e_c^- \rightarrow (Fe^{2+})^*$ (via electron capture) in n-type materials, and $Fe^{3+} \rightarrow (Fe^{2+})^* + h_v^+$ in SI material. The latter process was also observed by Klein and Weiser[11] using time-dependent PL measurements with below-gap excitation in SI-GaP:Fe. It was also concluded that the photoionized hole remained bound to the Fe center: $Fe^{3+} \rightarrow [Fe^{2+}]^* \cdot h_b$. It is also of interest to note that recent optically detected magnetic resonance (ODMR) measurements[12] in ZnSe:Fe indicate that even in the II-VI compounds electron capture by Fe^{3+} is involved in the excitation of Fe^{2+} PL.

II. EXPERIMENTAL

Sample growth and characterization will be described elsewhere[13] and will only be discussed briefly. A liquid-encapsulated Czochralski (LEC) Fe-doped boule, 2-77-*H*, was grown such that the small segregation coefficient[14] of the Fe left the seed end *n* type and left the tail end SI. Several slices were cut perpendicular to the (111) growth direction in order to avoid large gradients in the Fe concentration across each slice, and all samples studied were taken from the center of the appropriate slice. EPR measurements gave the Fe^{3+} concentration at 6 K on the SI side of the boule, and also helped determine the position of the *n*-type—SI transition. Hall-effect measurements were carried out for each slice at 300 and 77 K, and careful geometrical measurements gave the fraction of the melt that was solidified at that position in the boule. These data were analyzed in Ref. 13 to determine the equilibrium, low-temperature concentrations of Fe^{2+} and Fe^{3+} for each slice. This information appears in Table I, where the slices are labeled consecutively *A*—*I* from the seed to the tail end. The samples will be referred to in the rest of this paper as, e.g., sample *G*, or equivalently 2-77-*H*(*G*). At this point it will be useful to define some terminology. We will refer to samples with the equilibrium condition (at liquid-helium temperatures) $[Fe^{3+}] \gg [Fe^{2+}]$ as *overcompensated* (OC), and to samples with $[Fe^{+2}] \gg [Fe^{3+}]$ (or $[Fe^{3+}]=0$) as *partially compensated* (PC). Thus the SI sample 2-77-*H*(*I*) approaches the OC condition, the (mostly) *n*-type samples, 2-77-*H*(*A*—*G*) are PC, and 2-77-*H*(*H*) is intermediate (see Table I). Although these definitions appear somewhat arbitrary, they will be useful in discussing the time-dependent PL data which tend to exhibit different behavior for PC and OC samples rather than for strictly *n*-type or SI samples.

The samples were studied at temperatures between 2 and 300 K using a Janis Vari-Temp Dewar. The excitation source was a N_2-laser-pumped dye laser operating at 5800 Å with a pulse duration of 8 nsec and a repetition rate of 10—20 Hz. The dye-laser output was attenuated to allow ≈ 35 μJ/pulse incident energy on the sample, corresponding to an incident-power density of ≈ 300 kW/cm^2. Although this corresponds to a regime of high excitation, this density is still a factor of 2—3 below the threshold for laser oscillations,[8] so that this deformation of the PL time dependence was avoided. The 3.5-μm Fe^{2+} PL was collected with a spherical mirror and focused onto a cooled InSb detector ($\approx$30-nsec response). Either a $\frac{1}{4}$-m grating spectrometer or a 3.5-μm-longpass filter was used to isolate the signal due to Fe^{2+} PL. The amplified PL transient was recorded and signal averaged by a Tektronix 7912 AD transient digitizer, which was controlled by a microcomputer.

III. RESULTS

The time-dependent PL measurements to be presented were carried out either at fixed temperature as a function of sample position along the graded InP:Fe boule or for a given sample as a function of temperature. The results of

TABLE I. Properties of slices from the InP:Fe boule 2-77-*H* as determined by EPR and Hall-effect measurements and reported elsewhere (Ref. 13).

Sample 2-77-*H*( )	Fraction of melt solidified	ρ (Ω cm)		$n_D - n_A$ (cm^{-3})		μ (cm^2/V sec)		Equilibrium $[Fe^{3+}]$, $T \sim 6$ K (10^{15} cm^{-3})[a]	Equilibrium $[Fe^{2+}]$, $T \sim 6$ K (10^{15}cm^{-3})[b]
		300 K	77 K	300 K	77 K	300 K	77 K		
A	0.045	0.86	0.277	1.68×10^{15}	1.36×10^{15}	4336	16703		1.2
B	0.102	0.827	0.275	1.71×10^{15}	1.34×10^{15}	4428	16885		1.3
C	0.210	0.972	0.313	1.55×10^{15}	1.14×10^{15}	4156	17479		1.48
D	0.508	1.91	1.26	7.83×10^{14}	5.1×10^{14}	4168	9715		2.33
E	0.581	3.48	2.63	5.28×10^{14}	2.75×10^{14}	3399	8639		2.8
F	0.609	5.90	3.67	3.25×10^{14}	$\sim 2.8\times10^{14}$	3259	6060		2.95
G	0.632	22.5		2.25×10^{14}		1240		$\lesssim 0.055$	3.2
H	0.766	3.98×10^{6}		6.53×10^{8}		2403		1.29	3.85
I	0.957	1.32×10^{8}		3.02×10^{7}		1575		22.2	4.8

[a]EPR measurement, sensitivity $\approx 3\times10^{13}$ cm^{-3}.
[b]Deduced from EPR, Hall effect, and growth parameters.

the sample-dependent measurements suggest a relatively simple model for the relaxation of the system back to the equilibrium (dark) state in both n-type and SI samples. The temperature-dependent measurements give both qualitative and quantitative information about the recombination kinetics for times during as well as after the exciting laser pulse.

A. Sample dependence

The time dependence of the 0.35-eV $^5T_2 \rightarrow {}^5E$ PL intensity for eight samples is shown in the semilogarithmic plot in Fig. 1. All measurements were carried out at 4.2 K. The time response of the detection system to the exciting laser pulse is included in the inset. It should be emphasized that the duration of the exciting pulse (~ 8 nsec) as well as the recombination time ($\lesssim 1$ nsec) of the photoexcited carriers are both very short on the time scale of Fig. 1. Consequently, the time evolution of the PL response displayed in the figure occurs long after the exciting pulse has ended and the photoexcited electron-hole pairs have recombined. Thus, the time dependence of the PL intensity reflects the relaxation of the system back to the equilibrium (dark) state in response to the nonequilibrium condition generated by the exciting laser pulse.

There are several qualitative features of the data that are noteworthy. While all of the samples exhibit a similar (≈ 10-μsec) exponential decay at longer times, corresponding to the lifetime of the $^5T_2$ excited state, the PL response immediately after the exciting pulse varies considerably over the range of samples studied. The PL intensity from the OC sample I ($[Fe^{3+}] > > [Fe^{2+}]$) begins to decay immediately (to within the time resolution of the detection system) after the end of the exciting pulse, and exhibits a weak nonexponential component for $t \lesssim 1$ μsec (the exponential component is extrapolated by the dashed line). In contrast to this, all of the PC samples ($[Fe^{3+}] \ll + [Fe^{2+}]$) exhibit a *growth* in the PL intensity (and therefore of the population of the $^5T_2$ excited state) out to relatively long times ($\gtrsim 1$ μsec), until the slowing rate of growth is overtaken by the ≈ 10-μsec decay of the excited state. Exponential decay then sets in at longer times. Sample H exhibits intermediate behavior: Some growth is observed as with the PC samples, while a significant immediate PL response is also observed (as a "sharp corner" in the time dependence, as shown in the inset), similar to the OC sample I. Although there are no unam-

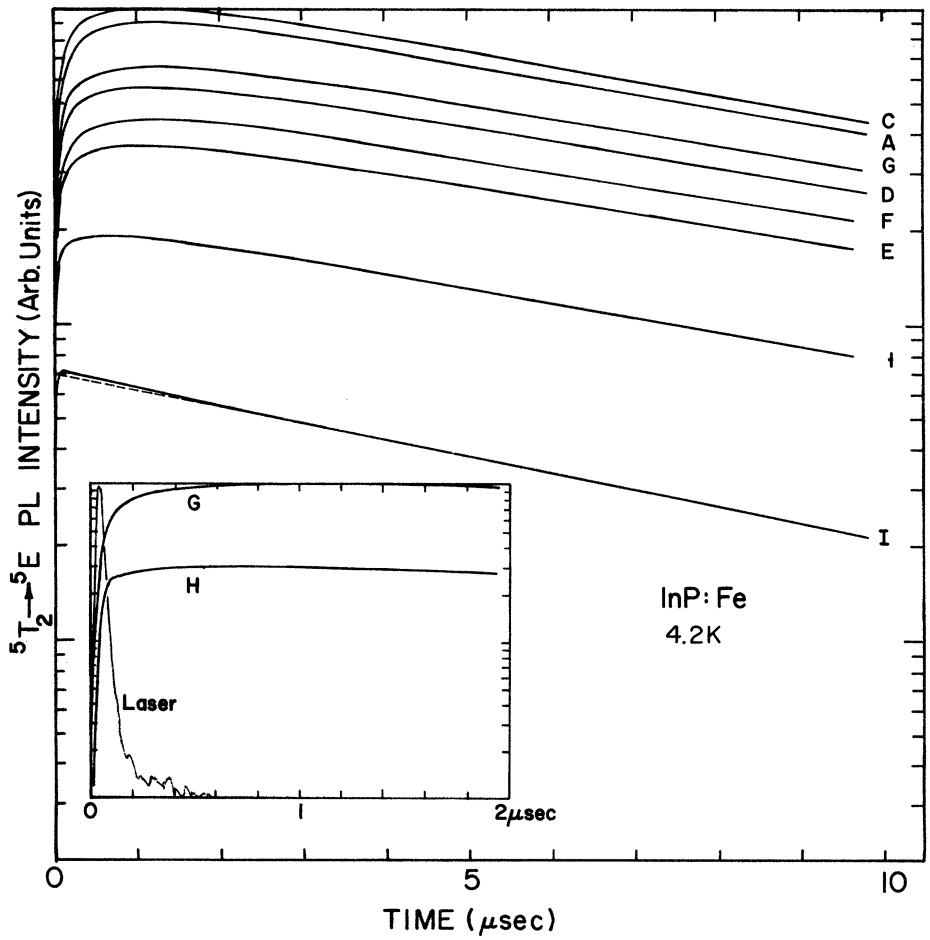

FIG. 1. Time dependence of the Fe^{2+} PL intensity for several InP:Fe samples from boule 2-77-H. Samples A–G are partially compensated, sample I is overcompensated, and sample H is intermediate, as explained in the text. The system response to the 8-nsec laser pulse is shown in the inset along with detailed data for samples G and H.

oiguous trends in the PL intensity within the set of PC samples, there is clearly a significant decrease in intensity from the PC samples to the intermediate sample H and from sample H to the OC sample I.

The data in Fig. 1 suggest a relatively simple picture for the excitation and recombination at the Fe center. This is shown in Fig. 2(a) for PC samples and in Fig. 2(b) for OC samples. Note that the position of the Fe^{3+} level in the gap is only *schematic*: It is not suggested that the position of this level relative to the band edges is known. For the PC samples the left-hand side of Fig. 2(a) indicates that essentially all of the Fe is in the Fe^{2+} ground state (^5E) before the exciting pulse ($t < t_{\text{pulse}}$). During excitation with above-band-gap light ($h\nu > E_g$), a large photoexcited carrier concentration is created. The Fe^{2+} may capture a hole or may be directly photoionized by the exciting light. That is, we may have either

$$Fe^{2+} + h\nu \rightarrow Fe^{2+} + e_c^- + h_v^+ \rightarrow Fe^{3+} + e_c^- \quad (1)$$

or

$$Fe^{2+} + h\nu \rightarrow Fe^{3+} + e_c^- \ . \quad (2)$$

When the exciting pulse ends the photoexcited electron-hole pairs recombine rapidly (≤ 1 nsec), leaving the nonequilibrium situation depicted on the right-hand side of Fig. 2(a), consisting of an excess concentration of Fe^{3+} and an equal number of excess conduction-band electrons. The system relaxes back to the equilibrium state via electron capture by the neutral Fe^{3+} center, creating Fe^{2+}. Capture is assumed to occur preferentially into the Fe^{2+} excited state since there is 0.35 eV less energy to dissipate. As only less than about 10^{15} cm^{-3} Fe^{3+} are typically involved in the capture process, the characteristic time for the capture can be relatively slow (≈ 200 nsec in these samples), as reflected in the relatively slow growth of the PL intensity (Fig. 1) after the end of the exciting pulse. As time increases, the rate of growth of the $^5T_2$ population slows since the Fe^{3+} concentration diminishes and the decay of the Fe^{2+} excited state begins to dominate the PL time dependence. Thus a maximum occurs in the PL intensity at the point where the growth of the $^5T_2$ population is balanced by the decay to the ground state.

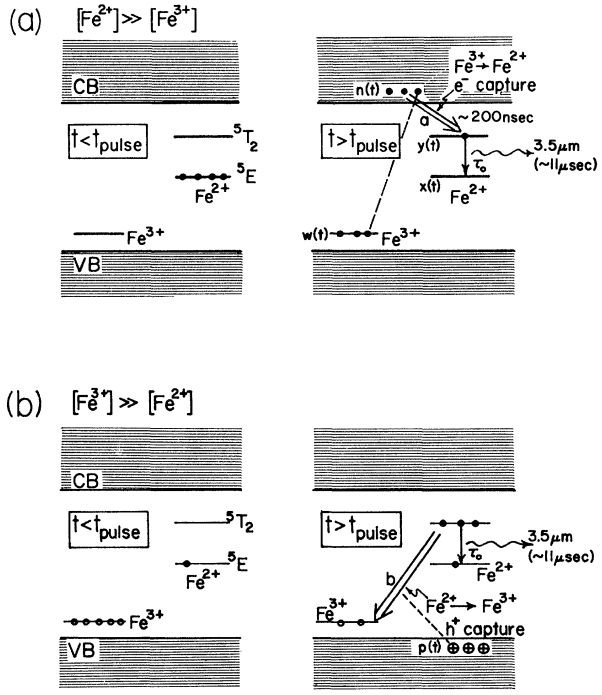

FIG. 2. A model to account for the kinetics of the excitation and recombination processes occurring after excitation with a short, intense pulse of above-band-gap light for (a) PC samples and (b) OC samples. The left-hand side of the figure corresponds to the equilibrium condition, while the right-hand side corresponds to the nonequilibrium state just after the end of the exciting pulse. The concentrations of various levels and the parameters associated with carrier capture and the $^5T_2$ lifetime are indicated on the figure in accordance with the discussion in the text. It should be noted that the Fe^{3+} level is only drawn schematically: We do not suggest that the position of this level relative to the band edges is known.

The analogous considerations for the OC sample are shown in Fig. 2(b). Here the equilibrium state $[Fe^{3+}] \gg [Fe^{2+}]$ shown on the left-hand side of the figure is considerably different than for the PC samples. It is just this difference that is responsible for the very different PL response that is observed (Fig. 1) for the two types of material. For the OC samples the dominant capture process under above-band-gap excitation is very likely the capture of free electrons by Fe^{3+}, thus producing excited Fe^{2+},

$$Fe^{3+} + h\nu \rightarrow Fe^{3+} + e_c^- + h_v^+ \rightarrow (Fe^{2+})^* + h_v^+ \ . \quad (3)$$

Therefore, after the exciting pulse ends and the photoexcited electron-hole pairs rapidly recombine, the system is left in a nonequilibrium condition [shown on the right-hand side of Fig. 2(b)] consisting of an excess concentration of Fe^{2+} and an equal number of valence-band holes. The system relaxes back to equilibrium via Coulombic hole capture by the Fe^{2+}. Since the capture process can occur while the Fe^{2+} center is either in the ground or the excited state, the relaxation process itself can compete with the radiative $^5T_2 \rightarrow {}^5E$ transition. This should be contrasted with the situation for PC samples, Fig. 2(a), where the relaxation of the system to equilibrium actually produces the Fe^{2+} excited state and thus the subsequent $^5T_2 \rightarrow {}^5E$ PL. It should be noted that for the OC samples the model in Fig. 2(b) contains no channel for increasing the Fe^{2+} excited-state concentration after the exciting pulse ends: The PL intensity will begin to decay immediately after the end of the exciting pulse and will exhibit no slow growth. In addition, the PL decay should exhibit a nonexponential component due to the competing hole capture by Fe^{2+} ($^5T_2$). It might also be concluded that since the relaxation of the system via hole capture competes with the PL transition, the PL intensity in OC samples should be weaker than for PC samples. Although the data in Fig. 1 exhibits this kind of behavior, the magnitude of the nonexponential component in the PL decay of sample I (Fig. 1) is too small to explain the large difference in intensity between OC and PC samples. This will be treated in more detail in a later section, where the observed inten-

sity differences will be discussed in terms of Auger processes occurring *during* the exciting pulse.

B. Temperature dependence

The analysis of the data presented in the preceding section will yield information about the magnitude of the important parameters governing the kinetics of the system, i.e., capture cross sections, excited-state lifetimes, and the initial concentrations of the various charge states at the end of the exciting pulse. In addition, by studying the temperature dependence of the time-dependent Fe^{2+} PL, we can also determine the temperature dependence of these parameters and thereby obtain information about the specific physical processes associated with them. Temperature-dependent measurements were carried out on three representative samples, 2-77-*H* (*A*, *G*, and *I*). Since the data for samples *A* and *G* are quite similar, only data

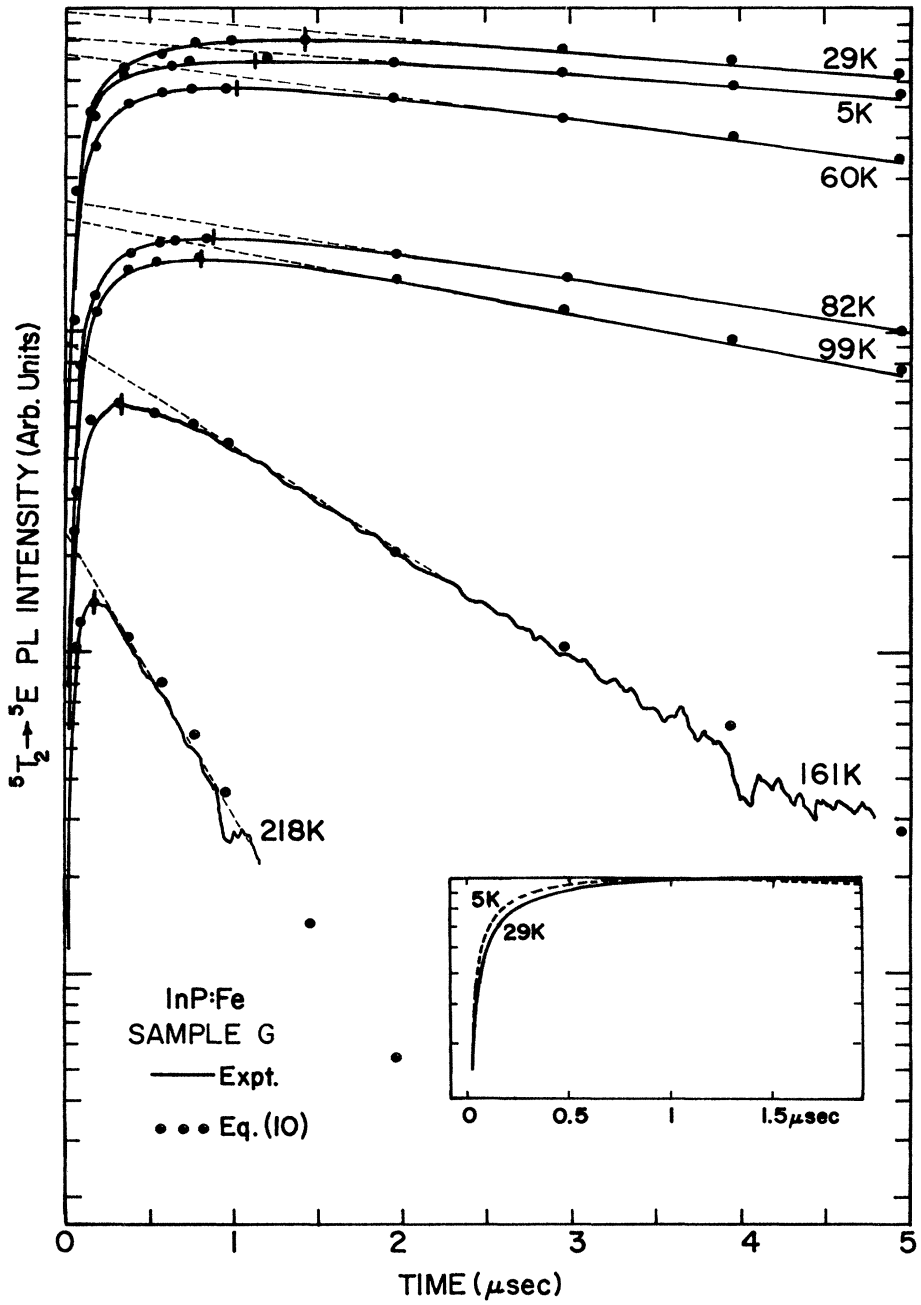

FIG. 3. Time dependence of the Fe^{2+} PL intensity for the PC sample 2-77-*H* (*G*) as a function of temperature. The closed circles are the result of a fit of this data to Eq. (10), and the dashed lines give the extrapolation of the long-time behavior back to $t=0$. The maximum of each data set is indicated by a vertical line through the data. The 5- and 29-K data are shown normalized to the same peak intensity in the inset, where it is clear that the rate of growth of the intensity (and therefore the $^5T_2$ population) is slower for the 29-K data.

for samples G and I will be shown explicitly. However, the data anlaysis for all three samples will be presented in the next section.

The temperature dependence between 5 and 218 K for the PC sample 2-77-$H(G)$ is shown in Fig. 3. The most obvious response to increasing temperature is the increasing decay rate at long times as well as the decrease in the overall intensity. Both are expected as a result of the increased efficiency of nonradiative (NR) transitions between the excited ($^5T_2$) and ground (^5E) states of Fe^{2+}. However, there is also a marked decrease in the intensity of the long-time behavior extrapolated to $t=0$ (the dashed lines in the figure) which will be related in the next section to the concentration of Fe^{3+} at the end of the exciting pulse (for PC samples). A more subtle feature of the data is observed in the time and the intensity of the maximum in the PL response. We recall that the maximum occurs at the time where the growth of the $^5T_2$ population due to electron capture is just balanced by the decay due to the $^5T_2$ lifetime. As the latter decreases at higher temperature the maximum shifts to shorter time, as observed in the data for $T \geq 60$ K. But between 5 and 29 K the time of the peak (indicated as a vertical line through the data) shifts gradually to *longer* time with increasing temperature. This is also emphasized by the data shown in the inset, where the 5- and 29-K data have been normalized to the same peak intensity: The slower growth of the 29-K data is obvious. In addition, the intensity of the maximum *increases* with increasing temperature, while the intensity for the $T \geq 60$ K data decreases. It should be pointed out that data for 10, 18, and 44 K all lie between the 5- and 29-K data, but were not included in the figure in order to avoid confusion between closely spaced data points. The shift of the peak to longer times with increasing temperature between 5 and 29 K (a temperature regime where the $^5T_2$ lifetime is approximately constant) indicates that the electron-capture process is slowing down with temperature. A decrease in the capture rate with increasing temperature is not expected from a multiphonon capture process by a deep level, and is, in fact, more characteristic of thermalization of carriers captured by a *shallow* level. This point will be discussed in more detail in a later section.

The temperature dependence of the time-dependent PL for the OC sample 2-77-$H(I)$ is shown in Fig. 4 for temperatures between 5.5 and 300 K. The main features of these data are the increased NR $^5T_2 \rightarrow {}^5E$ exponential decay rate and the decreased intensity with increasing temperature. In addition, a weak nonexponential decay component (presumably due to NR hole capture) is observed at lower temperatures (≤ 47 K) but is not detectable due to the increasing decay rate for $T \geq 60$ K. In the following subsection the weak contribution due to hole-capture processes is shown to be an indication that the system is not far from equilibrium after the exciting pulse: This is clearly a condition that results from the details of the kinetics during the pulse. Close examination of the data in Fig. 4 also reveals that the intensity extrapolated to $t=0$ also decreases with increasing temperature. In the next section this quantity is related to the $^5T_2$ concentration at the end of the exciting pulse. The observed temperature dependence will be related to the temperature dependence of the $^5T_2$ lifetime.

C. Data analysis

In this section we develop a quantitative model based on the ideas introduced in the preceding section: These are summarized by Figs. 2(a) and 2(b) for the PC and OC samples, respectively. The data presented above will be analyzed within the framework of this model to yield more detailed information about the parameters controlling the system kinetics. The model represented by Fig. 2 is the simplest picture that can account for the qualitative features observed in the data (Fig. 1) and that also makes good sense physically. It should also be pointed out that the physics of the excitation-recombination process at the Fe center will be shown to be quite different for the PC and OC samples. For PC samples excitation of the PL transition occurs primarily *after* the exciting pulse, and the relaxation of the system tends to *populate* the Fe^{2+} excited state. For OC samples, however, the excited state is populated *during* the exciting pulse, and the system relaxation tends to *compete* with the PL transition.

The models in Fig. 2 apply only for times after the end of the exciting laser pulse and after the photoexcited carriers have recombined: $t=0$ thus corresponds to the end of the laser pulse. Therefore, the nonequilibrium concentrations of Fe^{3+} and Fe^{2+} at the end of the pulse will be taken as parameters that correspond to the initial values of the time-dependent variables. As with most modeling procedures, some approximations must be assumed, and these are clearly indicated.

We first consider the case for PC samples. The time-dependent concentrations of Fe^{3+}, the Fe^{2+} (^5E) ground state, and the Fe^{2+} ($^5T_2$) excited state are labeled $w(t)$, $x(t)$, and $y(t)$, respectively. The electron-capture coefficient is a, τ_0 is the $^5T_2$ lifetime, and $n(t)$ is the concentration of excess conduction-band electrons. The rate equations describing the relaxation of the system back to equilibrium are

$$\dot{w}(t) = -an(t)w(t) , \tag{4}$$

$$\dot{y}(t) = an(t)w(t) - y(t)/\tau_0 , \tag{5}$$

$$\dot{x}(t) = y(t)/\tau_0 . \tag{6}$$

In addition, for times after the laser pulse, $n(t)=w(t)$. With the initial conditions $w(t=0)=w_0$ and $y(t=0)=y_0$, the solution to this set of equations is

$$w(t) = w_0/(1+aw_0t) , \tag{7}$$

$$y(t) = y_0 e^{-t/\tau_0} + w_0 e^{-t/\tau_0} \times \int_0^t e^{t'/\tau_0} a w_0 (1+aw_0 t')^{-2} dt' . \tag{8}$$

Numerical integration can be avoided by solving Eq. (8) for times $t \ll \tau_0$. The exponential inside the integral may then be approximated as unity, and Eq. (8) becomes

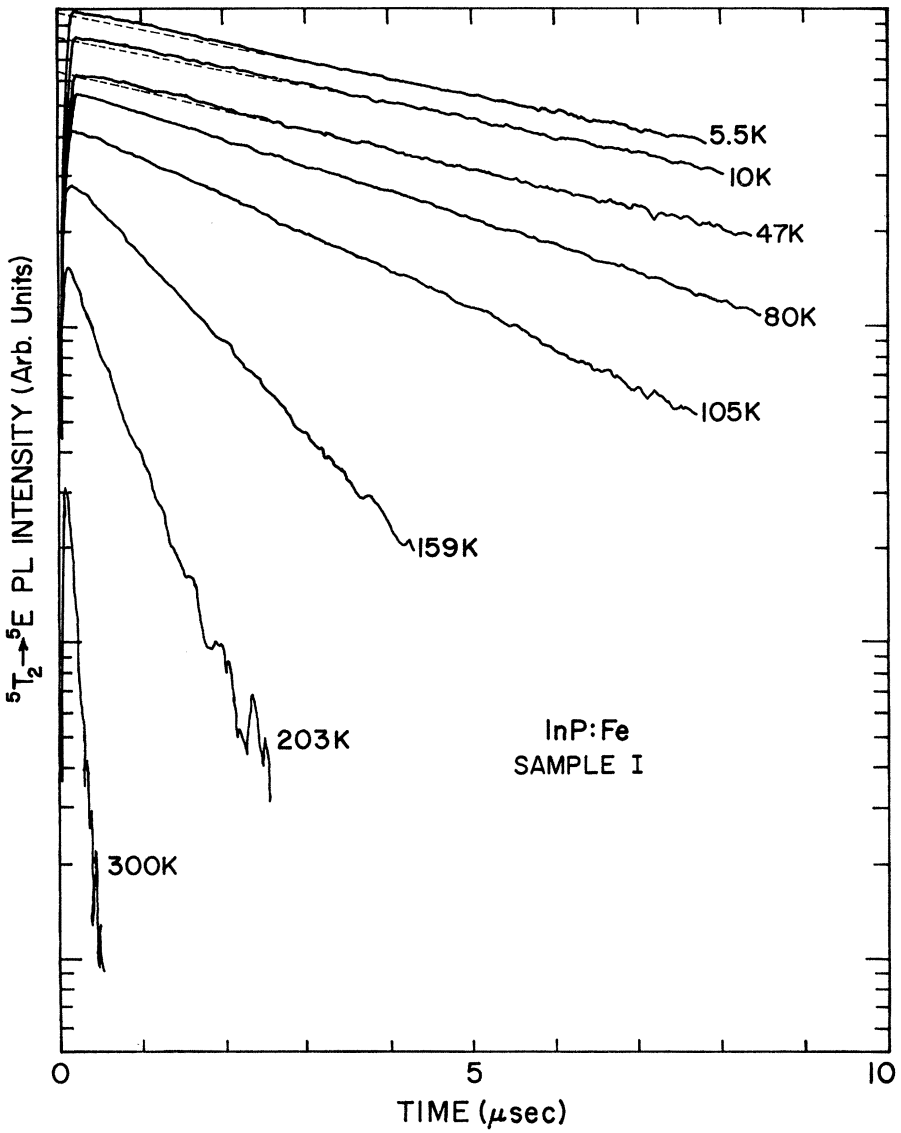

FIG. 4. Time dependence of the Fe^{2+} PL intensity for the OC sample 2-77-$H(I)$ as a function of temperature. The dashed lines represent the extrapolation of the long-time exponential decay to $t=0$. The small deviation of the data from this line at short times emphasizes the weak nonexponential component due to nonradiative hole-capture processes.

$$y(t)\cong y_0 e^{-t/\tau_0}+w_0 e^{-t/\tau_0} a w_0 t/(1+a w_0 t)\ . \tag{9}$$

The time-dependent PL intensity is proportional to $y(t)$. The term involving w_0 represents the electron-capture process shown in Fig. 2(a). The term involving y_0 represents radiative decay from the concentration of Fe^{2+} in the excited state at the end of the laser pulse, and results in immediate PL decay as discussed previously. This behavior is observed primarily in the OC sample and also in the intermediate sample H as a "sharp corner" in the data in Fig. 1. However, no such effect is observed in any of the PC samples. It is therefore assumed that in the PC samples this contribution is small compared to that due to the electron-capture process. With this assumption Eq. (9) becomes

$$y(t)\cong w_0 e^{-t/\tau_0} a w_0 t/(1+a w_0 t)\ . \tag{10}$$

This expression may be used to fit the time dependence of the PL intensity for PC samples. We first define the slope on the semilogarithmic data in Figs. 1, 3, and 4 as $m\equiv d(\ln y)/dt=\dot{y}/y$. For long times ($a w_0 t \gg 1$), Eq. (10) becomes $y(t)\approx w_0 e^{-t/\tau_0}$, so that

$$m(t\rightarrow\infty)=-1/\tau_0\ . \tag{11}$$

It will be shown later that $a w_0 \approx (200\ \text{nsec})^{-1}$ and $\tau_0 \approx 10$ μsec, so that use of the long-time behavior of Eq. (10) is not inconsistent with the approximation $t \ll \tau_0$ that was imposed in deriving Eq. (9). Note that the long-time exponential decay extrapolated to $t=0$ gives the extrapolated value $y_{\text{ext}}=w_0$ Therefore one finds that the corresponding extrapolated PL intensity I_{ext} is proportinal to w_0. Finally, the peak of the PL data occurs for $\dot{y}=0$ at $t=t_p$. Applying this to Eq. (10) we obtain the condition

for the peak to be

$$aw_0=(\tau_0-t_p)/t_p^2 . \quad (12)$$

Thus we can obtain from the data for PC samples the quantity τ_0 determined from the long-time slope and the parameter aw_0 using Eq. (12). Note, however, that the parameter w_0 is still unknown. But the long-time PL intensity extrapolated to $t=0$ (the dashed lines in Fig. 3), $I_{\text{ext}} \propto y_{\text{ext}}$, was shown above to be proportional to w_0. Thus the temperature dependence of (aw_0) and w_0 may be obtained independently. Using the measured values of these two parameters, τ_0 and aw_0, we have compared the data in Fig. 3 (solid lines) for temperatures between 5 and 218 K with the corresponding calculated values from Eq. (10) (the solid circles). The fit is remarkably good for all temperatures considering the simplicity of the model. The largest discrepancies are observed at longer times, where the condition ($t \ll \tau_0$) is just beginning to break down, and also at very short times (<50 nsec), where the PL response is distorted by the response of the system. It should be emphasized that the two fitting parameters τ_0 and aw_0 were not varied freely to obtain a best fit, but were determined directly from the long-time slope and the time of the peak.

The temperature dependence of the fitting parameters aw_0 and w_0 is shown for samples G and A in the semilogarithmic plot versus $1/T$ in Figs. 5 and 6, respectively. It is noteworthy that these two parameters exhibit opposite temperature dependences. This will be discussed in a later section. The decrease in aw_0 with increasing temperature ($T<29$ K) just reflects the shift in the peak of the PL response to longer times that was observed in Fig. 3. By dividing the temperature-dependent values of aw_0 by $I_{\text{ext}}(T)$, which is proportional to $w_0(T)$, $a(T)$ may be determined to within a scaling factor. Although we do not know the magnitude of w_0 (the concentration of Fe^{3+} at the end of the pulse), which is necessary to determine this scaling factor, we can assume that the maximum in $I_{\text{ext}}(T)$ in Figs. 5 and 6 corresponds to $w_0(\text{max}) \leq [\text{Fe}]_{\text{total}}$, i.e., less than the total Fe content in the sample (which is known). By assigning $I_{\text{ext}}(\text{max})=w_0(\text{max})=[\text{Fe}]_{\text{total}}$, we can determine a *minimum* value for $a(T)$, defined as $a_{\text{min}}(T)$. This is plotted in Figs. 5 and 6, giving a lower bound to the capture coefficient as a function of temperature. It should be emphasized that this procedure should result in a reliable temperature dependence for $a(T)$. A rigid translation of the logarithmic scale to the proper position is the only difference between $a(T)$ and $a_{\text{min}}(T)$. The results of a similar analysis for PC sample 2-77-$H(A)$ is shown in Fig. 6. The capture coefficient is observed to decrease by a factor of 2–3 for both samples as the temperature is raised from 5 to 29 K. Above this temperature a_{min} increases rapidly. This unusual behavior will be discussed in some detail in the next section.

The temperature dependence of $1/\tau_0$ is shown in Fig. 7. The rapid increase at higher temperatures results from the increased NR $^5T_2 \rightarrow {}^5E$ transition rate.

We will now analyze the data from the OC sample 2-77-$H(I)$, which may be modeled following the physical picture suggested in Fig. 2(b). All of the variable names remain the same. In addition, b represents the capture coefficient for holes by Fe^{2+}, and is assumed to be the

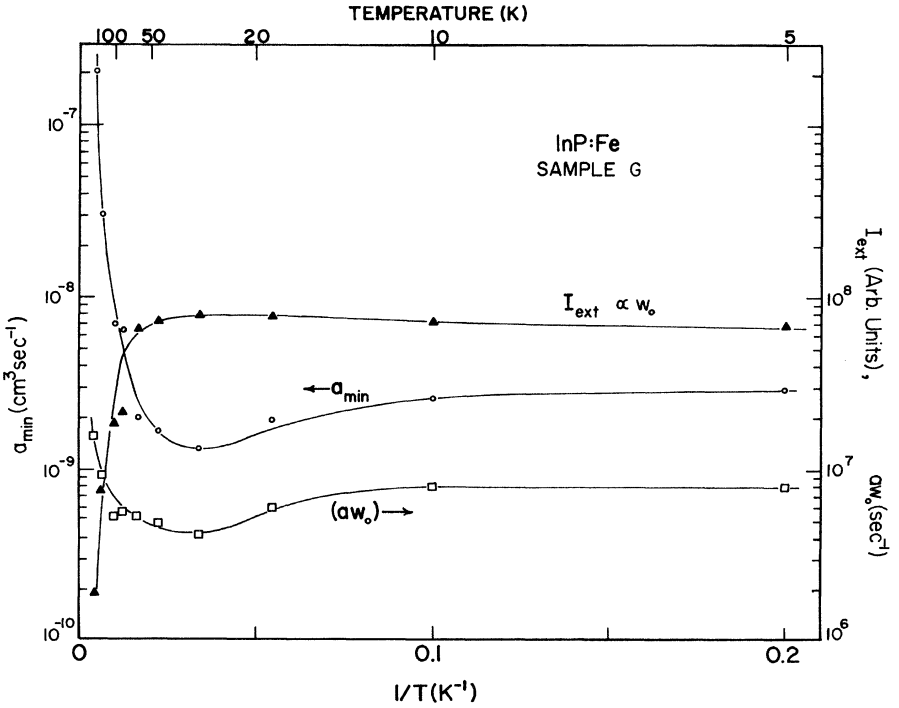

FIG. 5. Fitting parameter (aw_0), the extrapolated intensity I_{ext}, and a lower bound to the electron-capture coefficient a_{min} are plotted vs inverse temperature for sample 2-77-$H(G)$. The temperature dependence of a_{min} should reflect the correct temperature dependence of the capture coefficient $a(T)$. a_{min} represents a lower bound to the magnitude of the capture coefficient.

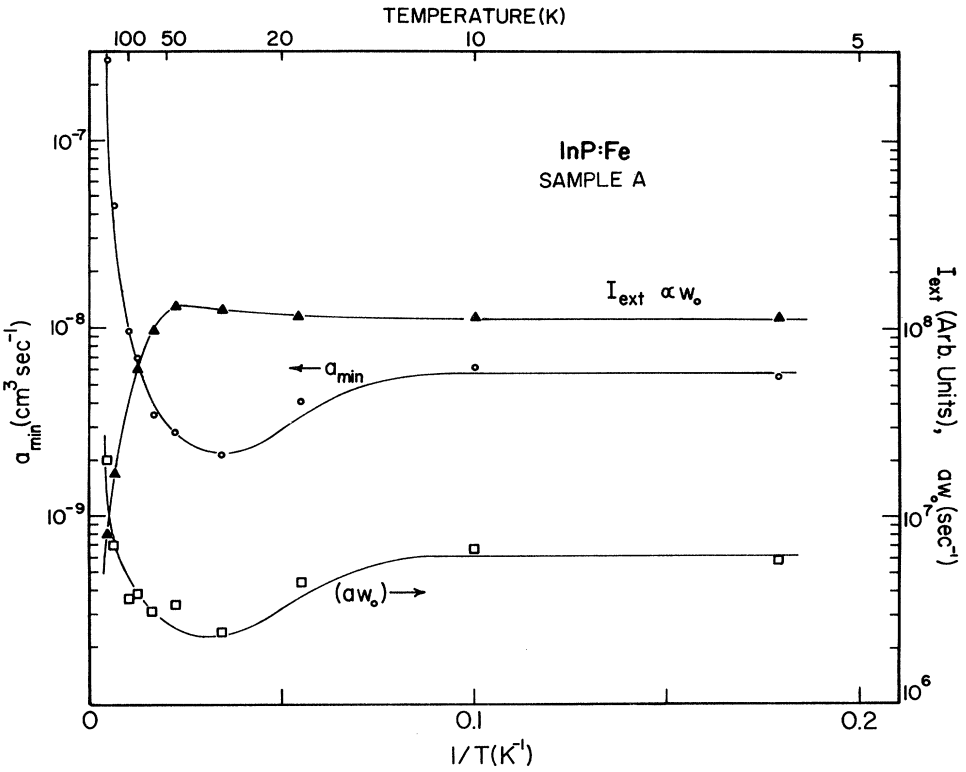

FIG. 6. PC sample 2-77-*H* (*A*). See the caption of Fig. 5.

same for both the Fe^{2+} excited and ground states. Since the magnitude of the capture coefficient is governed by the Coulombic nature of the capture, this is probably not a bad approximation. The nonequilibrium hole concentration is $p(t)$, and the population of the ground state Fe^{2+} (^5E) is x_0 at the end of the exciting pulse and x_e before the exciting pulse. The equilibrium Fe^{2+} concentration x_e in SI material is just the number of compensated donors and is known from characterization measurements (see Table I). The set of rate equations describing the relaxation of the system in Fig. 2(b) for times after the exciting pulse has ended and after the photoexcited carriers have recombined is given by

$$\dot{y}(t)=-y(t)/\tau_0-bp(t)y(t)\ , \tag{13}$$

$$\dot{x}(t)=y(t)/\tau_0-bp(t)x(t)\ , \tag{14}$$

with

$$p(t)=x(t)+y(t)-x_e\ . \tag{15}$$

Equation (15) simply states that the excess hole concentration must just balance the nonequilibrium Fe^{2+} concentration. Defining the total initial Fe^{2+} concentration as $z_0=x_0+y_0$, the solution of Eqs. (13)–(15) is

$$y(t)=y_0 e^{-t/\tau_0}[z_0/x_e-(z_0/x_e-1)e^{-bx_e t}]^{-1}\ . \tag{16}$$

Again defining $m=d(\ln y)/dt$, we find

$$m(t\to\infty)=-1/\tau_0,\quad m(t\to 0)=-1/\tau_0-bx_e(z_0/x_e-1)\ . \tag{17}$$

Also the extrapolation of the long-time behavior to $t=0$ gives

$$y_{ext}(t\to 0)=(x_e/z_0)y_0\ , \tag{18}$$

whereas from Eq. (16) we obtain

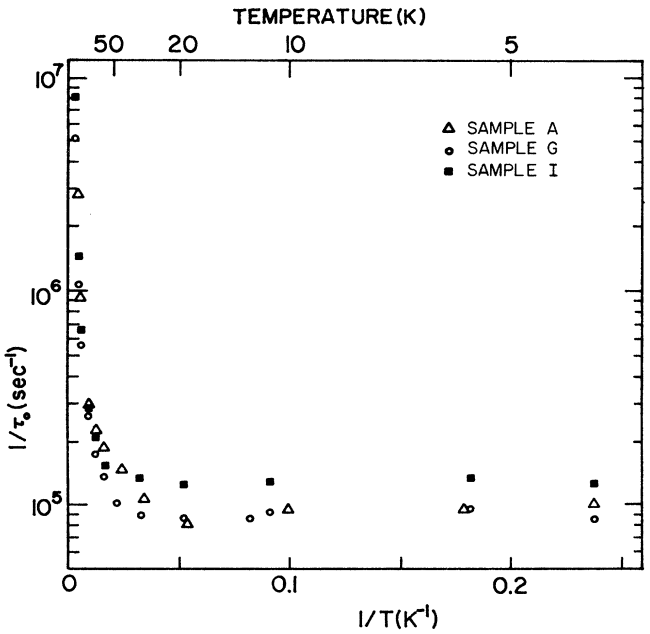

FIG. 7. Inverse $^5T_2$ lifetime is plotted as a function of inverse temperature for samples 2-77-*H* (*A*, *G*, and *I*).

$$y(t=0)=y_0 \ . \tag{19}$$

The ratio y_0/y_{ext} can be obtained directly from the data in Fig. 4 (the extrapolated intensity is determined by the dashed line), so that z_0/x_e may be measured directly from the data. Since the extrapolated and the actual data are so close together due to the relatively weak hole capture, z_0/x_e cannot be measured with great accuracy. From Eq. (17), a measurement of the difference between the slope in the data for $t\rightarrow 0$ and $t\rightarrow\infty$ gives $bx_e(z_0/x_e-1)$. Since z_0/x_e was determined independently and x_e is known from characterization, a value for b can be determined. This is plotted versus $1/T$ in Fig. 8, and is relatively constant over the temperature range studied, with $b\approx 7\times 10^{-11}\,\text{cm}^{-3}\,\text{sec}^{-1}$. The scatter in the data results primarily from the inaccuracy in determining z_0/x_e. Dividing b by the thermal velocity gives a capture cross section for holes at low temperature, $\sigma_p\approx 2\times 10^{-17}$ cm^2. Deep-level transient spectroscopy (DLTS) measurements by Lang and Logan[15] for GaAs:Fe give $\sigma_p\approx 1\times 10^{-16}$ cm^2 for $T>250$ K, which is in reasonable agreement. Also, the value z_0/x_e, which represents the ratio of the total Fe^{2+} concentration after the pulse to that before the pulse, was found to be only about 1.03. This indicates that the system was not left very far from equilibrium ($z_0/x_e=1$) after the exciting pulse. Thus the excess hole concentration (z_0-x_e) is low and the nonexponential component in the decay is small, as observed in the data. The temperature dependence of $y_0(T)$ is reflected in $I(t=0,T)$, which is also plotted in Fig. 8. The observed temperature dependence is discussed in the next section in terms of the temperature dependence of τ_0 which is plotted in Fig. 7 and is similar to that measured for the PC samples.

In summary, the time-dependent data for both PC and OC samples have been analyzed quantitatively in terms of a relatively simple model for the excitation-recombination process. From this procedure we have extracted the magnitudes and/or the temperature dependences of the important parameters that govern the system kinetics (capture coefficients, the $^5T_2$ lifetime, and the initial concentrations of the various Fe charge states). In the next section these results will be interpreted to give more detailed information about the physical processes that dominate the kinetics of the system.

IV. DISCUSSION

A. Process occurring after the exciting pulse: Electron capture by Fe^{3+}

The important processes occurring after the end of the exciting pulse are (see, e.g., Fig. 2) electron capture by Fe^{3+} (PC samples), hole capture by Fe^{2+} (OC samples), and the decay (radiative and NR) of the $^5T_2$ excited state of Fe^{2+}. Most of this section will be concerned with electron capture by Fe^{3+}, for which we will present evidence for the involvement of a shallow level in the capture process.

The first indication of the occurrence of a shallow intermediate state is given by the temperature dependence of the electron-capture coefficient shown in Figs. 5 and 6 for PC samples G and A, respectively. The capture coefficient is observed to decrease by about a factor of 2—3 as the temperature is raised from 5 to 29 K. Above this temperature, a_{min} increases rapidly. The decrease in the deep-level capture coefficient with increasing temperature is quite unexpected, as the multiphonon capture coefficient is expected to be independent of temperature in this

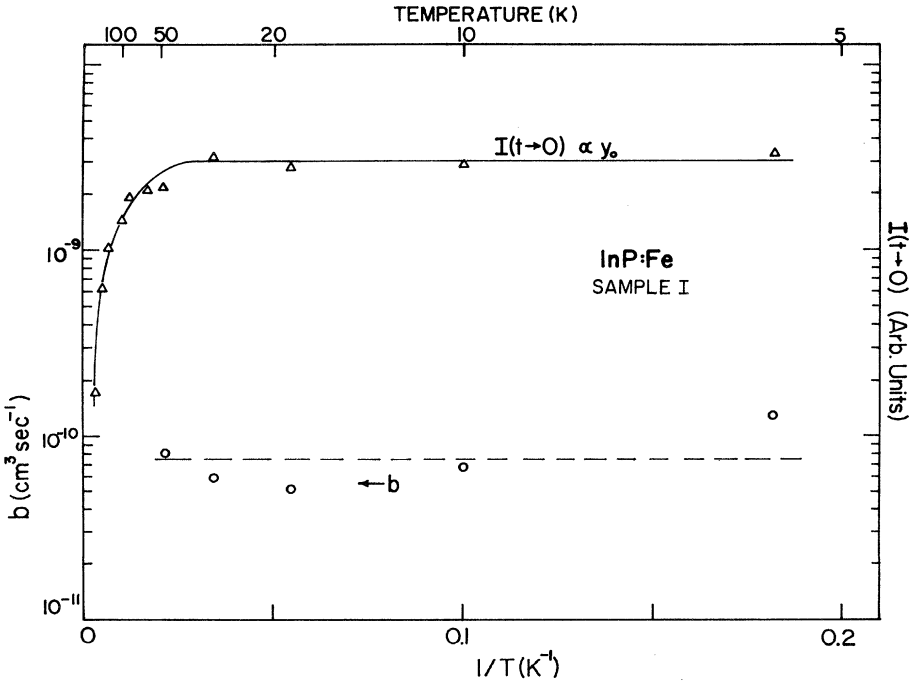

FIG. 8. Hole capture coefficient b and the maximum PL intensity $I(t\rightarrow 0)$ is plotted vs inverse temperature for OC sample 2-77-$H(I)$. The dashed line gives an average value for b at low temperature.

low-temperature regime and then to increase exponentially at higher temperature.[16] However, this type of behavior is expected from capture into a *shallow* level,[17] where at sufficiently high temperatures the captured carrier is thermalized back into the band, resulting in a decrease in the capture coefficient. At this point it is convenient to define a minimum electron-capture cross section by dividing the capture coefficient $a_{\min}$ by the thermal velocity $\langle v_{\rm th}\rangle=(3kT/m_e^*)^{1/2}$. The resulting $\sigma_n^{\min}$ gives a lower bound to the capture cross section, and is plotted in Fig. 9 for the two PC samples 2-77-$H(G)$ and 2-77-$H(A)$. Several values for σ_∞ determined by DLTS measurements[6,18,19] for Fe-related traps with levels near 0.64 eV in InP have also been included in the figure and are quite consistent with the values for $\sigma_n^{\min}$ determined by our time-dependent PL experiments. In addition, the *magnitude* of the low-temperature cross section at ~ 5 K is in the range 10^{-16}–10^{-15} cm^2. This is an enormous cross section for electron capture by a neutral deep level at low temperature. For purposes of comparison, electron capture by Fe^{3+} in GaAs was measured by Lang and Logan[15] above 250 K and by Kleverman *et al.*[20] for temperatures as low as 100 K. The measured cross section was found to be relatively temperature independent at low temperature with the value $\sigma_n \approx 10^{-19}$ cm^2. Thus the capture cross section in InP is 3–4 orders of magnitude larger than that for the same center in GaAs. The magnitude of the observed cross section is quite reasonable, however, for low-temperature capture by a neutral *shallow* level. This, in addition to the observed decrease in the capture coefficient with increasing temperature (also typical of capture by a shallow level), leads us to suggest that a shallow level may be involved in the electron-capture process by the deep Fe^{3+} center. In fact, a similar two-step capture process involving a shallow and a deep level was proposed by Gibb *et al.*[21] in connection with capture at a deep charged impurity. The model of Gibb *et al.* as applied to InP:Fe is shown in Fig. 10. According to this model, capture occurs into a shallow level and the captured carrier may be either thermalized back into the band or captured by the deep level by the process labeled ν, which may be temperature independent (e.g., radiative) or activated. At low temperature a carrier trapped by the shallow level will essentially always be captured by the deep level, so that the cross section for capture into the deep level will be equal to the cross section for capture into the shallow level (i.e., large). As the temperature is raised the cross section decreases due to thermal excitation out of the shallow level. If the process ν is independent of temperature, σ will continue to decrease. If, however, the process is activated with an activation energy greater than the depth of the shallow level, then the cross section will eventually turn around and increase with temperature, exhibiting activated behavior. The latter is just what is observed in the present case. From the range of temperatures where a decrease in $\sigma_n^{\min}$ is observed, the depth of the appropriate shallow level can only be a few meV. Experiments are presently being designed to verify this hypothesis directly by PLE spectroscopy near 0.64 eV using a tunable *F*-center laser.

At this point we will also speculate on the nature of the shallow level. Recently Robbins *et al.*[22] have observed by

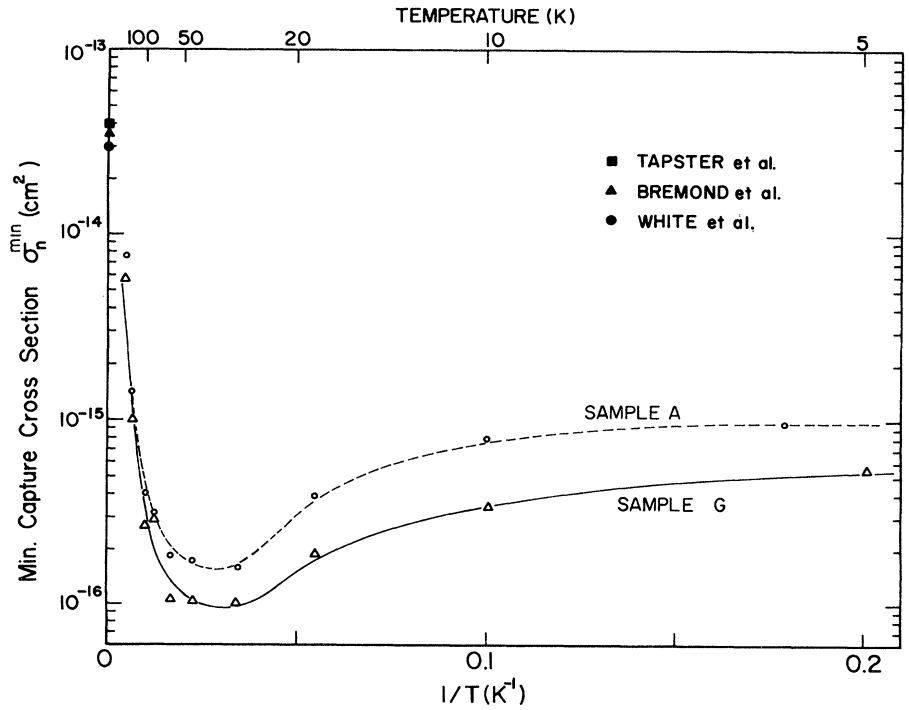

FIG. 9. Electron-capture cross section for Fe^{3+} derived from $a_{\min}(T)$ is plotted vs inverse temperature for two PC samples 2-77-$H(A$ and $G)$. The solid data points at $T\rightarrow\infty$ correspond to DLTS determinations of σ_∞ for this level and are consistent with the temperature dependences for samples A and G as determined by the fitting procedure described in the text.

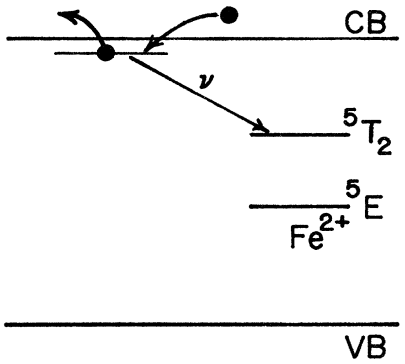

FIG. 10. Two-step electron-capture process proposed in Ref. 22 as applied to InP:Fe. Carriers trapped in the shallow level will be captured into the deep level at low temperatures and will be thermalized into the band at high temperatures. The shallow level in InP:Fe could be a charge-transfer state consisting of an electron split off from a conduction-band minimum and weakly bound to the Fe^{3+} center by the central-cell potential, as discussed in the text.

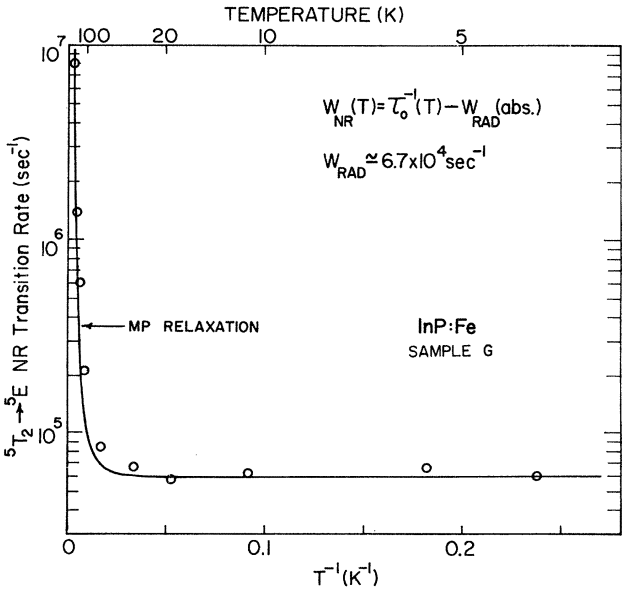

FIG. 11. Nonradiative component of the $^5T_2$ inverse lifetime is plotted vs inverse temperature for sample 2-77-*H*(*G*). The radiative rate was measured by absorption measurements, and the solid line represents the behavior expected due to multiphonon relaxation, as discussed in the text.

PLE spectroscopy a charge-transfer state in ZnSe:Co that consists of an electron weakly bound to Co^{3+} in a localized orbital that is split off from the conduction band and under the influence of the Co^{3+} impurity potential. The weakly bound electron state is denoted $[Co^{3+}]\cdot e_b$, emphasizing that the electron is weakly bound and that the Co is still in the Co^{3+} charge state. It is quite possible that a similar charge-transfer state exists for Fe^{3+} in InP, i.e., $[Fe^{3+}]\cdot e_b$. While the binding of the electron to the Co^{3+} center (which is positively charged with respect to the ZnSe lattice) involves both Coulombic and central-cell contributions, electron binding to the neutral Fe^{3+} center in InP would only involve the central-cell potential and would consequently be expected to be weaker. The deep-level capture process labeled ν in Fig. 10 would then involve recombination of the weakly bound electron with the hole that is tightly bound on the Fe^{3+} core (a type of deep bound exciton).

The hole-capture process occurring after the exciting pulse in the OC sample was shown in the preceding section to be relatively weak due to the fact that the system was left close to equilibrium after the exciting pulse. Thus it is not the magnitude of the capture cross section (which was found comparable to that in GaAs) that determines the contribution of this process to the PL decay: It is, instead, controlled by the parameter z_0/x_e, the ratio of the total Fe^{2+} concentration after the exciting pulse to that before the pulse. But this parameter is determined by processes occurring *during* the exciting pulse. The fact that it is found close to unity (equilibrium) and therefore contributes very weakly to the PL decay is discussed in the next subsection.

The temperature dependence of the $^5T_2$ lifetime was shown in Fig. 7 for samples 2-77-*H* (*A*, *G*, and *I*). In Fig. 11 we plot the nonradiative component of $1/\tau_0(T)$ for sample *G*. This was obtained by subtracting the radiative decay rate of the $^5T_2$ state, estimated from 3.5-μm optical-absorption measurements[23] to be $\approx 6.7\times10^4$ sec^{-1} ($\sim$15-μsec lifetime). The solid line through the data is a fit assuming relaxation via multiphonon emission, where a minimum number of local-mode phonons (observed in PL as phonon sidebands) were used to effect the loss of 0.35 eV. The only adjustable parameter is a scaling factor. From this fit it is reasonable to conclude that the temperature dependence of the $^5T_2$ decay is probably dominated by multiphonon emission. Although Auger processes (to be discussed in the next section) can also induce NR $^5T_2\rightarrow{}^5E$ transitions, the fact that both the PC and OC samples in Fig. 7 exhibit similar behavior indicates that the Auger process is not important after the exciting pulse for these samples. This effect will be shown to be important for more heavily *n*-type samples in the next section.

B. Processes occurring during the exciting pulse

It was noted earlier that the data in Fig. 1 showed that the PL intensity of the OC sample was an order of magnitude weaker than that of the PC samples, even though the latter have an order of magnitude lower Fe concentration. In attempting to understand this observation, it is worthwhile to restate the fact that within the models and the approximations introduced in the preceding section, the intensity from the PC samples is scaled by the concentration of Fe^{3+} at the end of the exciting pulse w_0, while the intensity from the OC sample is scaled by the concentration of excited $Fe^{2+}(^5T_2)$, y_0, at the end of the exciting pulse. These parameters are determined by the kinetics of the system *during* the exciting pulse. Although treating this problem analytically is considerably more complex than the relaxation back to equilibrium that was considered earlier, a qualitative discussion can still be quite

useful. Exciting a semiconductor with a short (8 nsec), high peak-power pulse (≈ 300 kW/cm^2) of above-band-gap light invariably produces a dense electron-hole plasma: In InP the carrier density[24] is $\gtrsim 10^{17}$ cm^{-3}. Processes that are dependent upon carrier concentration can therefore become particularly important during the exciting pulse. One such process that we have neglected thus far is Auger recombination.

There are, of course, many variations of Auger processes. In the present case three-particle processes resulting in electron-hole recombination are expected to be important in determining the carrier lifetime within the dense plasma. Recently, however, Langer[25] has suggested that Auger processes may be important in quenching radiative recombination at localized impurities at relatively modest carrier concentrations. Application of this model to transition-metal and rare-earth impurities in CdF_2 has been quite successful.[25] The process as applied to the Fe^{2+} center is shown schematically in Fig. 12. In the presence of carriers, the $^5T_2 \rightarrow {}^5E$ Fe^{2+} transition may occur nonradiatively, transferring the transition energy 0.35 eV to a conduction-band electron. The Auger rate is proportional to the carrier concentration through the Auger coefficient C_A:

$$1/\tau_A = C_A n \ . \tag{20}$$

For the InP:Fe system C_A has been estimated[26] to be $C_A \approx 6.7\times 10^{-10}$ cm^3 sec^{-1}. Although this process could have a measurable effect after the exciting pulse in PC samples, where there is a (time-dependent) concentration of excess electrons, the effect *during* the exciting pulse should be dramatic. With $n \approx 10^{17}$ cm^{-3}, Eq. (20) gives $\tau_A \approx 15$ nsec $\ll \tau_0$. Thus during the 8 nsec exciting pulse the Fe^{2+} excited state can be efficiently depopulated to the ground state by this process. With these considerations it is easy to see why the intensity of the OC sample is so much weaker than that of the PC samples: The Auger quenching only applies to the internal deexcitation of the Fe^{2+} charge state during the pulse and tends to diminish y_0. There is no effect on the Fe^{3+} concentration, and w_0 is unaffected.

There is further evidence that suggests that the Auger process suggested by Langer is effective in InP:Fe. The time dependence of the Fe^{2+} PL for a relatively *heavily-doped* n-type sample taken from a different boule is shown in Fig. 13. The boule, 1-66-*H*, was both Fe and Sn doped with $n_D - n_A \approx 4\times 10^{16}$ cm^{-3}. The overall PL intensity is weak, and the decay is rapid and very nonexponential. The decay rate even at the longest times measured is ≈ 3 μsec, much shorter than the $^5T_2$ lifetime in SI or moderately n-type samples. This behavior is just what would be expected from the effect of this Auger process on the PL decay.

We can obtain additional qualitative information about the dominant processes occurring during the exciting pulse by considering the transfer between the Fe^{2+} and Fe^{3+} charge states during the pulse. We recall that in both the PC and OC samples this transfer results in the populating of the excited state of Fe^{2+} and therefore produces the observed radiative emission. Three processes that effect this tranfer have been mentioned: They are electron capture at Fe^{3+} ($Fe^{3+} \rightarrow Fe^{2+}$) and hole capture and photoionization at Fe^{2+} ($Fe^{2+} \rightarrow Fe^{3+}$). An estimate of the characteristic lifetimes of both of these charge states during the exciting pulse can give some useful information about the kinetics during the pulse without carrying out a full calculation of the time evolution of each charge state concentration. For $T \approx 5$ K, using $n \cong p \approx 10^{17}$ cm^{-3}, $a \geq a_{\min} \approx 2\times 10^{-9}$ cm^{-3} sec^{-1} (Fig. 5), and $b \approx 7\times 10^{-11}$ cm^{-3} sec^{-1} (Fig. 8), we obtain the characteristic times for the first two processes, which are $\tau_e \equiv (an)^{-1} \lesssim 5$ nsec and $\tau_h \equiv (bp)^{-1} \approx 150$ nsec. Although the energy dependence of the photoionization cross section for Fe^{2+} in InP has been determined,[10] the *magnitude* of the cross section has not been measured. Kleverman *et al.*[20] have attempted such a measurement in GaAs:Fe; however, they were only able to obtain an upper bound $\sigma_n < 10^{-20}$ cm^2. The appropriate time constant associated with the Fe^{2+} photoionization is then $\tau_n = (\sigma_n F)^{-1}$, where the incident photon flux in our experiments is $F \approx 10^{24}$ cm^{-2} sec^{-1}. If σ_n in InP and GaAs are comparable then

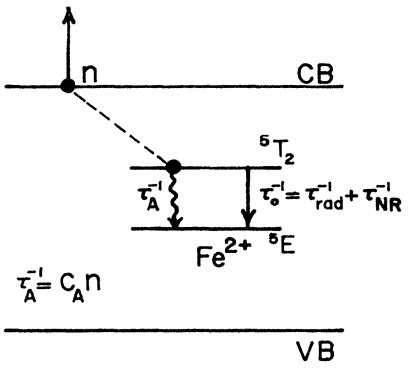

FIG. 12. Schematic of the Auger process suggested by Langer that can quench the Fe^{2+} luminescence. The Auger rate is proportional to the concentration of conduction electrons.

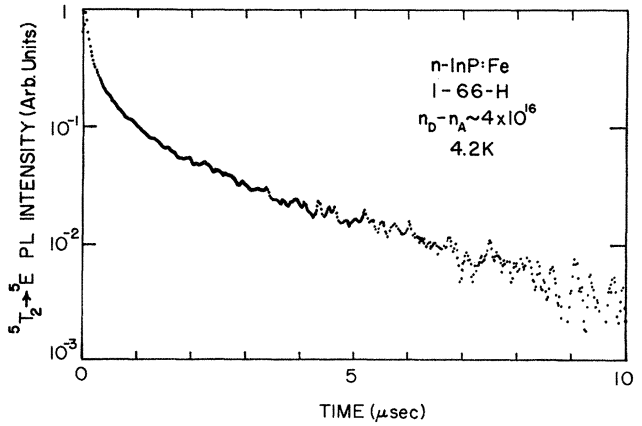

FIG. 13. Time dependence of the Fe^{2+} PL for a more heavily n-type InP:Fe boule 1-66-*H*. Note that the decay is quite nonlinear and that the $^5T_2$ lifetime at long times is ≈ 3 μsec, much shorter than for any of the 2-77-*H* samples at comparable temperatures (e.g., Fig. 7). This behavior is quite consistent with the increased importance of Auger processes for this sample.

we find $\tau_n > 100$ μsec. Since τ_h was estimated to be 3 orders of magnitude smaller than this value the appropriate Fe^{2+} lifetime is dominated by hole capture. The fact that the Fe^{3+} lifetime is $\tau_e < 5$ nsec indicates that in the PC samples (mostly Fe^{2+} before the pulse) the Fe^{3+} created during the pulse tends to converted rapidly back to Fe^{2+} due to the large capture cross section for electrons. This presents a contradiction, however, since the very same samples have exhibited laser oscillations from the $^5T_2 \rightarrow {}^5E$ transitions for times after the exciting pulse at only a factor of 3 higher excitation intensity than in the present measurements. This indicates that a sizable Fe^{3+} concentration must exist at the end of the pulse, since the population of the upper laser level ($^5T_2$) was found[8] to be due to $Fe^{3+} \rightarrow Fe^{2+*}$ electron capture after the exciting pulse. No laser oscillations were observed during the exciting pulse. The contradiction is resolved, however, when we consider that the origin of the large low-temperature electron-capture cross section is the postulated involvement of a shallow level in the capture process. During the exciting pulse, an electron bound by only a few millielectron-volts will be efficiently screened by the dense electron-hole plasma, and the enhanced electron-capture mechanism will be destroyed. The capture process will then proceed by, e.g., multiphonon emission, and the cross section can be expected to be typically 3 orders of magnitude smaller. Thus τ_e is of the order of 5 μsec during the pulse, and the photoexcited Fe^{3+} concentration is relatively stable until the exciting pulse ends. We may view this as indirect evidence of the involvement of a shallow level in the electron capture process.

These considerations may also be applied to the processes occurring in OC samples during the exciting pulse. It was noted earlier that the weak contribution of hole capture to the PL decay is due to the fact that the system is not far removed from equilibrium, $z_0/x_e \approx 1.03$. That the system is not excited far from equilibrium can be understood from the fact that $\tau_e \approx 5$ μsec during the pulse: Since τ_e is quite slow, very few $Fe^{3+} \rightarrow Fe^{2+*}$ charge transfers can occur during the 8-nsec pulse.

The temperature dependence of y_0, the excited Fe^{2+} concentration at the end of the pulse, was presented for the OC sample *I*, in Fig. 8, and exhibited a marked decrease at higher temperatures. The Auger effect cannot be responsible for this behavior, since the temperature dependence of the Auger effect is introduced only through the carrier concentration, which is determined by the optical excitation conditions in this SI sample. An increased hole capture rate, which would be expected at higher temperature, would decrease the total Fe^{2+} concentration. But since the system was shown to be very close to equilibrium after the pulse ($z_0/x_e \approx 1.03$), this effect could only decrease z_0/x_e toward 1 and would not account for the large decrease in intensity ($z_0/x_e < 1$ was not observed, since this corresponds to a regime with excess *electrons*, and would result in *growth* of the PL with time, as observed in the PC samples). The observed temperature dependence of y_0 is most probably due to an increased $^5T_2 \rightarrow {}^5E$ nonradiative transition rate during the pulse. The $^5T_2$ lifetime τ_0 was shown to decrease markedly at higher temperatures for all three samples shown in Fig. 7, and the temperature range of the increase corresponds to the decrease observed in y_0 (Fig. 8). Thus, from the good agreement between the data in Fig. 11 and multiphonon relaxation, it is not unreasonable to conclude that the temperature dependence of y_0 is probably also due to nonradiative multiphonon relaxation between the $^5T_2$ and ^5E states.

In PC samples a similar decrease at high temperature was observed in w_0, the Fe^{3+} concentration at the end of the pulse. This effect clearly cannot have the same origins as the decrease of y_0 at high temperature, since the $^5T_2 \rightarrow {}^5E$ transition has little or no effect on w_0. However, since the temperature dependence of the Fe^{3+} electron capture cross section becomes activated at high temperature (even without the involvement of a shallow level in the capture process), during the pulse $Fe^{3+} \rightarrow Fe^{2+}$ transitions will be more efficient, thus resulting in a smaller concentration w_0 at the end of the pulse. This can be seen in Figs. 5 and 6, where the capture coefficient $a_{\min}$ and w_0 exhibit the opposite sense of variation with temperature.

V. SUMMARY

From the analysis of the experimental data presented above we have gained a rather detailed understanding of the dominant processes governing the excitation and recombination kinetics at the Fe center in InP. This exemplifies the power of time-resolved experiments as applied to deep centers: In the present case a generally complete picture of the transitions associated with Fe has been developed. Specifically, the time dependence of the $^5T_2 \rightarrow {}^5E$ Fe^{2+} photoluminescence transition in InP has been measured as a function of temperature for a series of Fe-doped samples ranging from *n* type to SI. Qualitative differences between the time dependences observed in samples with $[Fe^{2+}] \gg [Fe^{3+}]$ and samples with $[Fe^{3+}] \gg [Fe^{2+}]$ were attributed to the different nonequilibrium states induced in the two types of materials by the exciting laser pulse: Excess Fe^{3+} and an equal number of conduction band electrons resulted in the former case while excess Fe^{2+} and an equal number of valence-band holes resulted in the latter. This simple model was also found to fit the experimental time dependences quite well over a wide range of temperatures. The fitting procedure yielded the magnitudes and/or temperature dependences of the parameters governing the system kinetics.

The low-temperature capture cross section for electrons by Fe^{3+} was found to be very large ($> 5 \times 10^{-16}$ cm^2) for capture by a neutral center, and more than 3 orders of magnitude larger than the comparable parameter in GaAs. This coupled with the observed decrease in the electron-capture coefficient with increasing temperature between 5 and 29 K tends to suggest a two-step capture process involving carrier capture by a shallow level followed by capture into the deep level. It is speculated that the nature of the shallow level could be a charge-transfer state consisting of an electron weakly bound to Fe^{3+} and split off from a conduction-band minimum, in analogy with recent work by Robbins *et al.*[22] in ZnSe:Co.

The low-temperature capture cross section for holes by Fe^{2+} ($\sim 2 \times 10^{-17}$ cm^2) was found to be in reasonable agreement with that in GaAs, and for low-temperature

Coulombic deep-level capture generally. The $^5T_2$ lifetime, ≈ 11 μsec for $T \leq 10$ K, exhibited a temperature dependence that was consistent with increased nonradiative decay due to multiphonon emission.

In addition, the temperature dependence of the Fe^{2+} and Fe^{3+} concentrations at the end of the laser pulse gave information about the system kinetics *during* the pulse. For example, it was concluded that an Auger process effective in quenching luminescence at localized impurities was expected to be particularly important during the exciting pulse, when the carrier density is high.

ACKNOWLEDGMENTS

The authors would like to thank J. Langer for several helpful discussions about the localized-impurity Auger effect, D. Paget for his critical reading of the manuscript, and K. Weiser, for his contributions during the initial phases of this work. This work was supported in part by the U.S. Office of Naval Research.

[1]G. K. Ippolitova, E. M. Omelyanovskii, N. M. Pavlov, A. Y. Nashelskii, and S. U. Yakobsen, Fiz. Tekh. Poluprovodn. 11, 1315 (1977) [Sov. Phys.—Semicond. 11, 773 (1977)].

[2]W. H. Koschel, S. G. Bishop, and B. D. McCombe, in *Proceedings of the 13th International Conference on the Physics of Semiconductors,* edited by F. G. Fumi (Tipografia, Marves, Rome, 1976), p. 1065.

[3]W. H. Koschel, U. Kaufmann, and S. G. Bishop, Solid State Commun. 21, 1069 (1977).

[4]S. G. Bishop, P. B. Klein, R. L. Henry, and B. D. McCombe, in *Semi-Insulating III-V Materials,* edited by G. J. Rees (Shiva, Orpington, 1980), p. 161.

[5]L. Eaves, A. W. Smith, M. S. Skolnick, and B. Cockayne, J. Appl. Phys. 53, 4955 (1982).

[6]P. R. Tapster, M. S. Skolnick, R. G. Humphreys, P. J. Dean, B. Cockayne, and W. R. MacEwan, J. Phys. C 14, 5069 (1981).

[7]P. Leyral, G. Bremond, A. Nouailhat, and G. Guillot, J. Lumin. 24/25, 245 (1981).

[8]P. B. Klein, J. E. Furneaux, and R. L. Henry, Appl. Phys. Lett. 42, 638 (1983).

[9]S. G. Bishop, in Deep Centers in Semiconductors, edited by S. T. Pantelides (Gordon and Breach, New York, in press).

[10]G. Bremond, A. Nouailhat, G. Guillot, and B. Cockayne, Solid State Commun. 41, 477 (1982).

[11]P. B. Klein and K. Weiser, Solid State Commun. 41, 365 (1982).

[12]K. P. O'Donnell, K. M. Lee, and G. D. Watkins, J. Phys. C 16, L723 (1983).

[13]P. B. Klein, R. L. Henry, T. A. Kennedy, and P. G. Siebenmann (unpublished).

[14]R. L. Henry and E. M. Swiggard, J. Electron. Mater. 7, 647 (1978).

[15]D. V. Lang and R. A. Logan, J. Electron. Mater. 4, 1053 (1975).

[16]R. Pässler, Phys. Status Solidi B 85, 203 (1978).

[17]H. Gummel and M. Lax, Phys. Rev. 97, 1469 (1955).

[18]G. Bremond, A. Nouailhat, G. Guillot, and B. Cockayne, Electron. Lett. 17, 55 (1981).

[19]A. M. White, A. J. Grant, and B. Day, Electron. Lett. 14, 409 (1978).

[20]M. Kleverman, P. Omling, L. Å. Ledebo, and H. G. Grimmeiss, J. Appl. Phys. 54, 814 (1983).

[21]R. M. Gibb, G. J. Rees, B. W. Thomas, B. C. H. Wilson, B. Hamilton, D. R. Wight, and N. F. Mott, Philos. Mag. 36, 1021 (1977).

[22]D. J. Robbins, P. J. Dean, C. L. West, and W. Hayes, Philos. Trans. R. Soc. London Ser. A 304, 499 (1982).

[23]P. B. Klein (unpublised).

[24]O. Hildebrand, E. O. Goebel, K. M. Romanek, H. Weber, and G. Mahler, Phys. Rev. B 17, 4775 (1978).

[25]J. Langer, in *Light Emitters and Detectors,* edited by M. Herman (Pergamon, New York, 1983), p. 303.

[26]J. Langer (private communication).